porization coefficient obtained by using the geometric area for A_1 was 0.0035 ± 0.0004 and was independent of temperature for the experimental range. The vaporization coefficient, α, is by definition the ratio of the free-evaporation and saturation fluxes, or

$$\alpha = J_{\text{free}}/J_{\text{satn}} \tag{5}$$

The coefficient at any particular temperature can, therefore, be directly obtained experimentally.

Preliminary free-evaporation fluxes were observed on the Mettler system using pressed pellets of $(SN)_x$ in thermal contact with graphite crucibles. The results in the form of Langmuir pressures are shown graphically in Figure 1, and the average value of α is 0.0024 ± 0.001, which is in reasonable agreement with that observed in the treatment above.

Discussion

The inherent accuracy of the direct Knudsen method for the determination of vapor pressure under saturation conditions in the molecular-flow regime is well recognized. However, there are numerous materials with very low vaporization coefficients where it is either impractical or impossible to construct cells for the attainment of saturation conditions. For materials of this type, the authors believe that the experimental techniques described in this paper for the treatment of Knudsen results at undersaturation can be used to obtain saturation pressures with accuracies approaching those inherent in the direct method. Vapor pressures for these materials are generally obtained using mass spectrographic techniques and accuracy is often limited by the lack of knowledge of fragmentation parameters and ionization cross sections.

The enthalpy of vaporization (32.49 kcal/mol) obtained in this study is in reasonable agreement with the value (29 kcal/mol) obtained by mass spectral techniques.[4] The value of the vaporization coefficient (0.0024) obtained directly with eq 5 from the free-evaporation measurement and that obtained from the analysis of the undersaturation data (0.0035) are not independent since the same saturation pressure is used in both cases. However, the authors believe that the agreement obtained does tend to validate the extrapolation technique and the simplifying assumption made in correlating the undersaturation data with the classical form of eq 1.

The heat of vaporization is, of course, a measure of the energy needed to break the bond between atoms in the bulk phase to give the species in the gas phase. The heat of vaporization, then, is often closely approximated by the bond strength between the atoms involved in the bond breakage. In the case of $(SN)_x$, there is a large discrepancy between the value of the heat of vaporization (30 kcal) and the S–N bond strength (~50–60 kcal).[13] Since the low vaporization coefficient suggests that the vapor species is in fact quite different from the bulk species, this seemingly large discrepancy can be understood. It is highly probable that some molecular rearrangement takes place which is exothermic to the extent of ~30 kcal. One possible example of such a process would be the formation of a cyclic equilibrium species with the formation of an S–N bond. The mass spectral data[4] appear to rule out the formation of an eight-membered ring, but other ring systems can be postulated. Although this study does not conclusively prove the formation of such a species, it does give evidence for the formation of a "nonlinear" structure in the gas phase at equilibrium.

Acknowledgment. The authors wish to thank Professor A. G. MacDiarmid for discussions throughout this work and for samples provided in the early stages of the investigation.

Registry No. $(SN)_x$, 37221-29-7.

References and Notes

(1) NRC–NRL Resident Research Associate, 1975–1977.

(2) (a) V. V. Walatka, Jr., M. M. Labes, and J. H. Perlstein, *Phys. Rev. Lett.*, **31**, 1139 (1973); (b) R. L. Green, P. M. Grand, and G. B. Street, *ibid.*, **34**, 89 (1975).

(3) A. A. Bright, M. J. Cohen, A. F. Garito, A. J. Heeger, C. M. Mikulski, P. J. Russo, and A. G. MacDiarmid, *Phys. Rev. Lett.* **34**, 206 (1975).

(4) R. D. Smith, J. R. Wyatt, J. J. DeCorpo, F. E. Saalfeld, M. J. Moran, and A. G. MacDiarmid, *J. Am. Chem. Soc.*, in press.

(5) A. A. Bright, M. J. Cohen, A. F. Garito, A. J. Heeger, C. M. Mikulski, and A. G. MacDiarmid, *Appl.* Phys. *Lett.*, **26**, 612 (1975).

(6) K. Motzfeldt, *J. Phys. Chem.*, **59**, 139 (1955).

(7) P. Clausing, *Ann. Phys.* (*Leipzig*), **12**, 961 (1932).

(8) T. D. Sandry and F. D. Stevenson, *J. Chem. Phys.*, **53**, 151 (1970).

(9) T. K. Basu and A. W. Searcy, *J. Chem. Soc.*, *Faraday Trans. 1*, **72**, 1899 (1976).

(10) H. G. Wiedmann, *Chem.-Ing.-Tech.*, **36**, 1105 (1964).

(11) C. T. Ewing and K. H. Stern, *J. Phys. Chem.*, **77**, 1442 (1973).

(12) C. M. Mikulski, P. J. Russo, M. S. Saran, A. G. MacDiarmid, A. F. Garito, and A. J. Heeger, *J. Am. Chem. Soc.*, **97**, 6358 (1975).

(13) L. Pauling, "The Nature of the Chemical Bond", 3rd ed, Cornell University Press, Ithaca, N.Y., 1960, p 82 f.

Contribution from Bell Laboratories,
Murray Hill, New Jersey 07974

Preparation and Properties of Li_xVS_2 ($0 \leq x \leq 1$)

D. W. MURPHY,* C. CROS, F. J. DI SALVO, and J. V. WASZCZAK

Received June 22, 1977 AIC704429

We report the preparation of Li_xVS_2 for $0 \leq x \leq 1.0$, this being the first report of the existence of VS_2. We present a partial phase diagram for this system based on x-ray diffraction measurements and differential scanning calorimetry. These measurements, as well as magnetic susceptibility measurements, show the existence of a number of phase transitions which are related to both the large crystallographic hexagonal c/a ratio and probable electronic instabilities in the V d band.

There is considerable current interest in van der Waals bonded metal chalcogenides and their compounds with lithium as potential cathodic electrodes in nonaqueous lithium batteries.[1,2] The group 4B and 5B MX_2 and $LiMX_2$ (X = S, Se) have been reported with the exception of VS_2.[3-5] It is surprising that VS_2 alone of these MX_2 compounds has not been prepared by direct combination of the elements especially since VSe_2 is readily prepared. In addition, only Li_xTiS_2 has been studied in any detail over the range of compositions $0 \leq x \leq 1$.[6] The compounds Na_xVS_2 ($0.3 \leq x \leq 1$) have been reported.[7] We report here a new method of delithiation of $LiVS_2$[8] and some simple physical properties of Li_xVS_2 ($0 \leq x \leq 1$).

Experimental Section

The $LiVS_2$ used was prepared as previously described[8] except that V_2O_5 was used instead of V_2O_3. Iodine solutions of ~0.2 N were prepared from freshly sublimed I_2 and acetonitrile freshly distilled from P_2O_5 and were standardized with thiosulfate. In the presence of acetonitrile, starch complexes with iodine did not form, but the color of the iodine itself was adequate and accurate as checked by

Table I

Compd	*T*, °C	*a*, Å	*c*, Å	*c*/*a*
VS_2	25	3.218	5.755	1.786
$Li_{0.10}VS_2$[a,b]	265	3.261	6.029	1.846
$Li_{0.25}VS_2$[b]	180	3.276	6.113	1.865
$Li_{0.33}VS_2$[b]	110	3.277	6.152	1.877
$Li_{0.40}VS_2$[a,b]	300	3.295	6.170	1.873
$Li_{0.50}VS_2$[b]	150	3.307	6.212	1.877
$Li_{0.55}VS_2$[b]	250	3.320	6.218	1.872
$Li_{0.60}VS_2$[b]	250	3.320	6.202	1.868
$Li_{0.66}VS_2$	250	3.342	6.196	1.853
	25	3.324	6.152	1.850
$Li_{0.75}VS_2$	200	3.359	6.180	1.839
	25	3.339	6.148	1.841
$Li_{0.90}VS_2$	200	3.398	6.133	1.804
	25	3.374	6.148	1.841
$Li_{1.0}VS_2$	45	3.39	6.10	1.799
	25	3.381	3 × 6.139	3 × 1.816

[a] Two phases at room temperature. [b] Structure distorted at room temperature; see text.

adding acetonitrile to a known concentration of aqueous triiodide. All Li_xVS_2 with $x < 1.0$ were prepared with a stoichiometric quantity of iodine solution which was entirely consumed (visually). VS_2 was prepared with a slight excess which was titrated after filtration. Atomic absorption spectroscopy confirmed the absence of Li in VS_2 and x-ray fluorescence the absence of iodine. Thermal gravimetric analysis confirmed the stoichiometry $V_{1\pm0.01}S_2$. The values of x in Li_xVS_2 are based on the amount of iodine added and are probably accurate to ±0.02–0.03. The $LiVS_2$ was treated with *n*-BuLi prior to use to ensure that maximum lithium content was attained. All reactions were run under Ar and all products containing Li were handled in an Ar atmosphere.

In a typical reaction, $LiVS_2$ (1.316 g, 10.79 mmol) was treated with 30 mL of I_2 (0.236 N, 7.08 mmol of I) and stirred. Within five minutes the solution was colorless; stirring was continued for ~16 h. The $Li_{0.33}VS_2$ product was filtered, washed with CH_3CN, and vacuum dried.

X-ray powder patterns were obtained either by the Debye–Scherrer method in sealed capillaries or by a diffractometer with the use of a holder which could be evacuated, and the sample was heated resistively on Pt foil to obtain high-temperature patterns. Magnetic susceptibility data were obtained by the Faraday method with samples sealed in quartz tubes. Differential scanning calorimetry (DSC) data were obtained on a Perkin-Elmer DSC-1B, using samples in pressure-sealed aluminum cans.

Results

The series Li_xVS_2 ($0 \leq x \leq 1$) was prepared by oxidation of $LiVS_2$ with iodine in acetonitrile according to eq 1. This

$$\mathrm{LiVS_2} + [(1-x)/2]\mathrm{I_2} \rightarrow \mathrm{Li}_x\mathrm{VS_2} + (1-x)\mathrm{LiI} \qquad (1)$$

oxidation is rapid and quantitative at room temperature. All the Li may be removed from $LiVS_2$ in a matter of minutes, depending on the stirring rate, since the reaction is heterogeneous. The highly colored I_2 solution becomes colorless upon completion of the reaction. Since the I_2/I^- couple is reversible, annealing of products was not necessary to obtain uniform Li content. In solvents such as CCl_4 where LiI is insoluble, the reaction did not proceed.

A number of compositions of Li_xVS_2 ($0 \leq x \leq 1$) were prepared by adding known aliquots of I_2 to $LiVS_2$ which had been previously treated with *n*-BuLi. (Most of our "$LiVS_2$" prepared at high temperature was approximately $Li_{0.95}VS_2$.) Magnetic susceptibility, x-ray, and DSC data are summarized in Figures 1–5 and Tables I–IV.

Table II. Crystallographic Data for VS_2

I(obsd)	*d*(obsd), Å	*d*(calcd), Å	*hkl*
100	5.735	5.7330	001
5	2.876	2.8765	002
2	2.784	2.7869	100
66	2.508	2.5081	101
41	2.002	2.0015	102
11	1.918	1.9172	003
13	1.610	1.6090	110
15	1.581	1.5798	103
5	1.551	1.5495	111
16	1.439	1.4382	004
6	1.355	1.3542	201
5	1.256	1.2540	202
3	1.151	1.1506	005
3	1.130	1.1273	203
7	1.073	1.0723	114
2	1.065	1.0635	105
3	1.036	1.0361	211
3	0.990	0.9891	212

Table III. Crystallographic Data for β-$Li_{0.50}VS_2$

β phase[a]				Hexag high-temp form	
I(obsd)	*d*(obsd), Å	*d*(calcd), Å	*hkl*[b]	*hkl*	*d*(obsd), Å
77	6.092	6.162	001	001	6.151
4	3.044	3.081	002	002	3.008
11	2.845	2.841	110	100	2.859
		2.632	$\bar{2}01$	101	2.5923
100	2.600	2.591	$\bar{1}11$		
		2.581	201		
54	2.564	2.574	111		
17	2.129	2.130	$\bar{2}02$	102	2.101
52	2.105	2.105	$\bar{1}12$		
42	2.067	2.078	112		
		2.076	202		
	1.692	1.692	$\bar{2}03$	103	1.675
14	1.651	1.651	203		
		1.655	310	110	1.654
56		1.640	020		
9	1.609	1.590	311	111	1.599
9	1.590	1.585	021		
15	1.537	1.540	004	004	1.550
9	1.404	1.409	$\bar{4}01$	201	1.397
12	1.287	1.287	222	202	1.302

[a] Calculated values for monoclinic cell; $a = 5.756$ Å, $b = 3.280$ Å, $c = 6.164$ Å, and $\beta = 91.28$ Å. [b] Bracketed indices of monoclinic cell arise from indicated hexagonal indices in adjacent column.

A neutron powder diffraction study[8] of $LiVS_2$ indicated a hexagonal unit cell with $a = 3.380$ Å and $c = 6.138$ Å, in good agreement with our values (Table I). We have observed (Figure 1j) a few weak extra lines in x-ray powder patterns which may be indexed as (001) lines from a 3c superlattice. We have observed a reversible transition (apparently first order) at 310 K in magnetic susceptibility (Figure 2), DSC (Figure 3), and x-ray patterns. The x-ray results (Figure 1i) indicate destruction of the superlattice above this transition.

The VS_2 prepared by this method is stable in air or Ar to 300 °C, beyond which S loss occurs. The compound is hexagonal (CdI_2 type) with $a = 3.217$ Å and $c = 5.745$ Å (Table II). A transition is observed in magnetic susceptibility and DSC at ~305 K. No change was observed in x-ray patterns above and below the transition. The transition is approximately a third as energetic as that of $LiVS_2$.

Compositions of Li_xVS_2 with $0.66 \leq x \leq 1.0$ give regular CdI_2 type hexagonal x-ray patterns at room temperature and above. The parameters are summarized in Table I and Figure 4, and the c/a ratio is given in Figure 5. The c/a ratio which is somewhat high for $LiVS_2$ (1.816 at 25 °C) actually increases with decreasing x and the c axis itself increases slightly over this range from 6.10 Å in $LiVS_2$ to 6.15 Å in $Li_{0.66}VS_2$, in contrast to Li_xTiS_2.[6] The transition present in $LiVS_2$ is not observed in $Li_{0.9}VS_2$ by x-ray diffraction but is detectable in $Li_{0.9}VS_2$ by DSC (Figure 3). At $Li_{0.75}VS_2$ no transition is observed above 215 K by DSC.

In the range $0.5 \lesssim x \lesssim 0.6$ the hexagonal unit cell is reduced in symmetry as indicated by splitting of a number of lines (Table III and Figure 1g). Above ~345 K the $Li_{0.5}VS_2$ cell

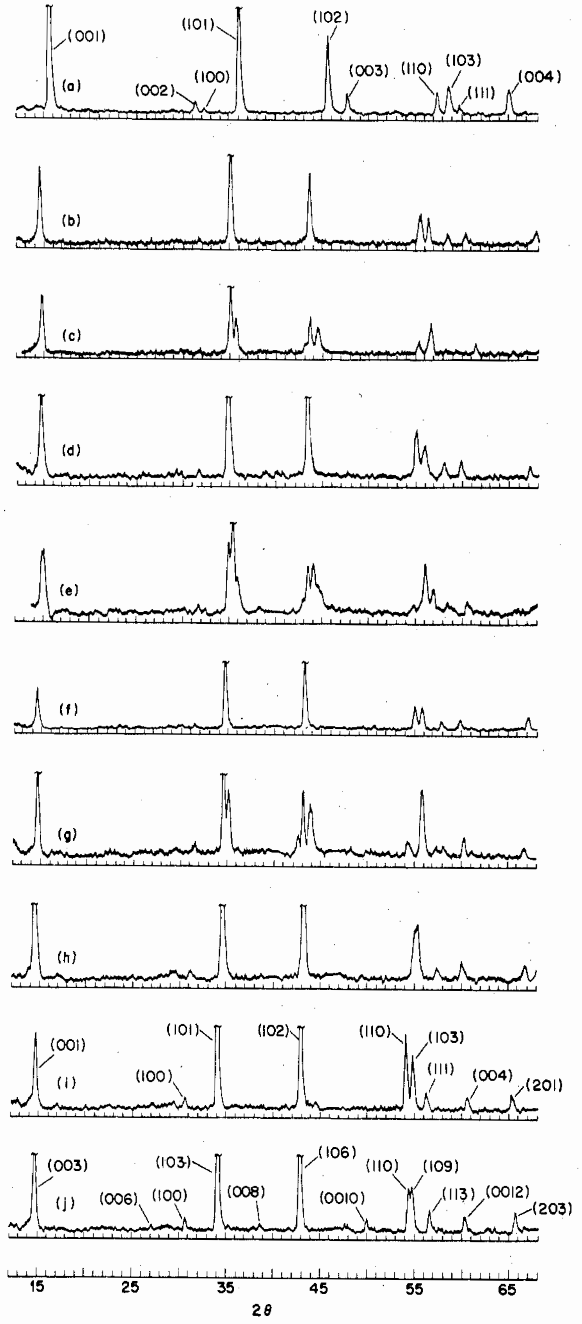

Figure 1. X-ray diffractograms of Li_xVS_2 obtained with Cu Kα radiation: (a) VS_2 (25 °C); (b) $Li_{0.33}VS_2$ (110 °C); (c) $Li_{0.33}VS_2$ (25 °C); (d) $Li_{0.4}VS_2$ (300 °C); (e) $Li_{0.4}VS_2$ (25 °C); (f) $Li_{0.50}VS_2$ (150 °C); (g) $Li_{0.50}VS_2$ (25 °C); (h) $Li_{0.66}VS_2$ (25 °C); (i) $Li_{1.0}VS_2$ (45 °C); (j) $Li_{1.0}VS_2$ (25 °C).

becomes hexagonal as indicated by the x-ray powder pattern (Figure 1f). The transition is also observed in magnetic susceptibility (Figure 2) and DSC (Figure 3) and is reversible. The distorted form (β in Figure 6) is best indexed for $Li_{0.5}VS_2$ as monoclinic with $a = 5.756$ Å, $b = 3.280$ Å, $c = 6.164$ Å, and $\beta = 91.28°$ (Table II). The unit cell is closely related to the hexagonal cell by $a \approx 3^{1/2}a_0$, $b \approx a_0$, and $c \approx c_0$ (a_0 and c_0 hexagonal parameters). The true unit cell is difficult to assess with powder data and must await single-crystal data to be certain.

For $0.25 \lesssim x \lesssim 0.33$ (α phase Figure 6) a distortion occurs which appears very similar to the β phase by x-ray measurements and is best indexed for $Li_{0.33}VS_2$ (Table IV) as monoclinic with $a = 5.659$ Å, $b = 3.240$ Å, $c = 6.050$ Å, and $\beta = 91.0°$. The magnetic susceptibility (Figure 2) and DSC

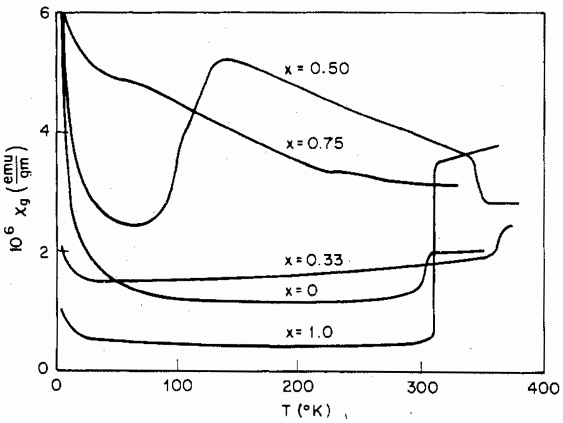

Figure 2. Magnetic susceptibility of Li_xVS_2.

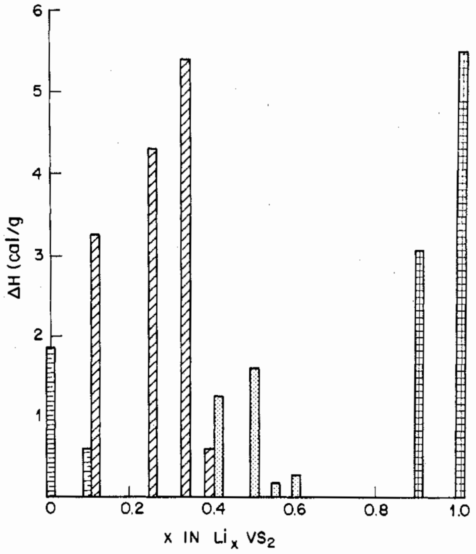

Figure 3. Differential scanning calorimetry (DSC) data for Li_xVS_2: ⊞, 3S → 1T, $T \approx 35–40$ °C; ▦, $\beta \rightarrow$ hexag 1T, $T = 65–70$ °C; ▨, $\alpha \rightarrow$ hexag 1T, $T = 75–90$ °C; ▤, $T \approx 30–35$ °C.

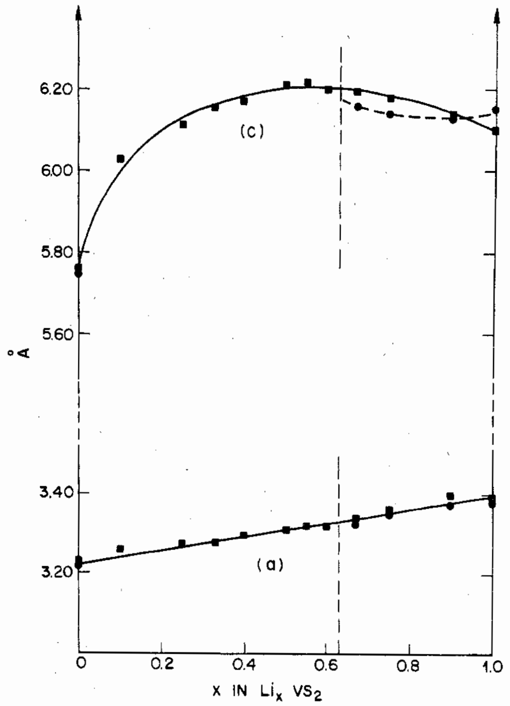

Figure 4. The hexagonal a and c parameters of Li_xVS_2 (from Table I): ■, high-temperature data; ●, room-temperature data.

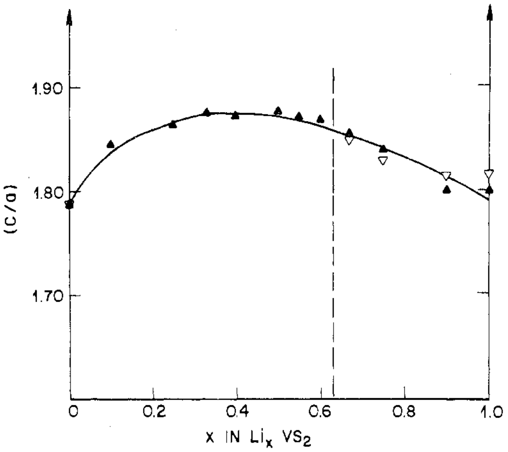

Figure 5. The c/a parameter of hexagonal Li_xVS_2: ▲, high-temperature data; ▽, room-temperature data.

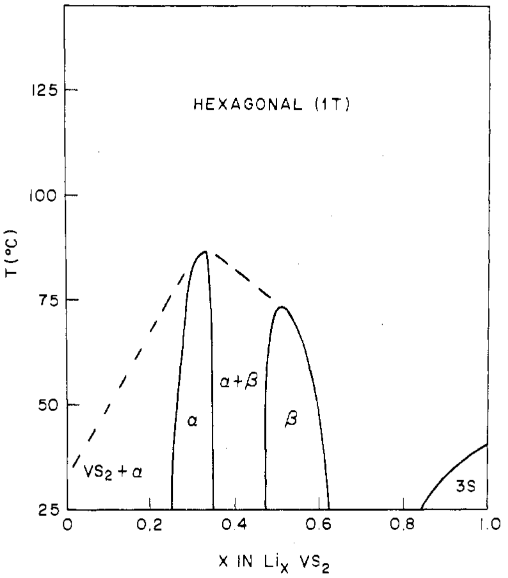

Figure 6. A partial phase diagram of the Li_xVS_2 system. The α and β phases are described as monoclinic.

Table IV. Crystallographic Data for α-$Li_{0.33}VS_2$

α phase[a]				Hexag high-temp form	
I(obsd)	d(obsd), Å	d(calcd), Å	hkl	hkl	d(obsd), Å
67	6.038	6.050	001	001	6.138
5	3.026	3.025	002	002	3.071
7	2.821	2.812	110	100	2.870
100	2.571	2.580	$\bar{2}01$	101	2.574
		2.558	$\bar{1}11$		
		2.546	201		
42	2.528	2.541	111		
10	2.107	2.131	210		
42	2.082	2.085	$\bar{2}02$	102	2.086
		2.068	$\bar{1}12$		
		2.051	112		
29	2.044	2.049	202		
15	1.666	1.656	$\bar{2}03$	103	1.662
		1.629	203		
36	1.631	1.630	310	110	1.639
		1.620	020		
4	1.590	1.580	$\bar{3}11$	111	1.584
4	1.564	1.568	311		
13	1.513	1.512	004	004	1.539
12	1.373	1.372	401	201	1.388

[a] Calculated values for monoclinic cell; $a = 5.659$ Å, $b = 3.240$ Å, $c = 6.050$ Å, and $\beta = 91.0°$.

(Figure 3) are quite distinct from the β phase. Evidence that the α and β distortions are distinct also comes from $Li_{0.40}VS_2$ which clearly shows both phases by x-ray (Figure 1e) and DSC (Figure 3) measurements. A two-phase region also exists between the α phase and Li_xVS_2 ($x \rightarrow 0$). The two-phase nature was observed in x-ray powder patterns and DSC data.

A partial phase diagram obtained from the data presented is shown in Figure 6. The positioning of the phase boundaries is approximate, and technically a two-phase region must separate the β and 1T phases from the 1T and 3S phases although we did not observe this.

Compositions of Li_xVS_2 ($x \geq 0.4$) are sensitive to moisture in the air and decompose with evolution of H_2S. For $x \approx 0.33$ water is intercalated to give a composition of $Li_{0.33}(H_2O)_{0.9}VS_2$ with a repeat layer spacing of 8.70 Å with no evolution of H_2S. We have been unable to index the full x-ray pattern, but this appears to be similar to the first-stage hydrated Na_xVS_2 observed by Wiegers.[7]

Discussion

The most striking aspect of the Li_xVS_2 system is the occurrence of the two slightly distorted phases α and β. A number of A_xMS_2 (A = Na, K, Cs) compounds exhibit structures[9] differing from those of the parent MS_2 compounds by translational orientation of the MS_2 layers with respect to each other. Differing translational orientations may be caused by ordering of the A ions or the preference of the A ion to become trigonal prismatic.[9] $NaVS_2(Se_2)$ undergoes a slight distortion below 50 K,[7] but no $LiMS_2$'s have been shown to exhibit such distortions. Several other compounds which may be regarded as metal intercalated MS_2's do show apparently similar distortions, e.g., V_5S_8 ($V_{0.25}VS_2$, monoclinic)[10] and $Ni_{0.25}TiS_2$ (monoclinic).[11]

The phase transitions in the Li_xVS_2 series appear to be related to electronic instabilities in the VS_2 layers. Such instabilities could take the form of a charge density wave (CDW),[12] as observed in many MX_2 layered compounds (including VSe_2), or some may be more similar to Mott-like transitions observed in vanadium oxides such as VO_2,[13] V_3O_5,[14] V_4O_7,[15] V_6O_{11},[15] and V_2O_3[16] (these compounds span the range from d^1 to d^2, as does Li_xVS_2 as x increases from 0 to 1). When both d^1 and d^2 V are present in the oxides, two transitions are frequently observed.

It seems likely that the distortion in VS_2 is due to a CDW as in VSe_2.[17-19] The transition in $LiVS_2$ may be more Mott-like as in V_2O_3 since the lattice of $LiVS_2$ is more ionic than that of VS_2. At intermediate compositions more complicated states likely exist, possibly with interactions between the electronic instabilities and the Li ions resulting in an ordering of the Li ions.

Thompson[20] has noted an empirical correlation between the crystallographic c/a ratio and the transition temperature of the CDW in layered MX_2's. The instabilities in compounds with high c/a ratios occur at higher temperatures. This relationship predicts a transition in VS_2 at 385 K, while the observed temperature is 305 K. The large c/a ratio of VS_2 and $LiVS_2$ becomes even larger (Figure 5) at intermediate compositions, and those compositions which form distorted structures at room temperature have a high-temperature hexagonal phase where $c/a \gtrsim 1.85$.

The magnetic susceptibility of $Li_{0.5}VS_2$ is very unusual. At the transition to the β distortion at 345 K, the magnetic susceptibility increases by 20% whereas with all other compositions the susceptibility decreases. Below this transition the susceptibility continues to increase with decreasing temperature, until a second transition near 140 K (and perhaps a third at 100 K) causes a marked decrease in susceptibility. A similar behavior has been observed in the magnetic susceptibility of Na_xVSe_2 ($0.3 \leq x \leq 0.6$).[21] Since the susceptibility above 350 K is only weakly temperature dependent, it appears that some V atoms develop magnetic moments below 345 K and that these couple antiferromagnetically or are lost again below 140 K.

The presence of these distorted phases gives rise to unusual electrochemical behavior as lithium is intercalated and deintercalated.[22]

Summary

We have prepared Li_xVS_2 for $0 \leq x \leq 1$, this being the first report of the existence of VS_2. All of the compositions show evidence for phase transitions near or below room temperature. These transitions are due, at least in part, to electronic instabilities of the V d band.

Acknowledgment. We are indebted to P. K. Gallagher for the TGA results and B. G. Bagley for assistance with the DSC data.

Registry No. VS_2, 12166-28-8; $Li_{1.0}VS_2$, 12218-74-5; $Li_{0.10}VS_2$, 64175-20-8; $Li_{0.25}VS_2$, 64175-16-2; $Li_{0.33}VS_2$, 64175-14-0; $Li_{0.40}VS_2$, 64175-18-4; $Li_{0.50}VS_2$, 64175-13-9; $Li_{0.55}VS_2$, 64175-22-0; $Li_{0.60}VS_2$, 64175-19-5; $Li_{0.66}VS_2$, 64175-15-1; $Li_{0.75}VS_2$, 64175-17-3; $Li_{0.90}VS_2$, 64175-21-9.

References and Notes

(1) M. S. Whittingham, *J. Electrochem. Soc.*, **123**, 315 (1976).

(2) D. W. Murphy and F. A. Trumbore, *J. Cryst. Growth*, **39**, 185 (1977).

(3) J. A. Wilson and A. D. Yoffe, *Adv. Phys.*, **18**, 193 (1969).

(4) M. B. Dines, *Mater. Res. Bull.*, **10**, 287 (1975).

(5) D. W. Murphy, F. J. Di Salvo, G. W. Hull, Jr., and J. V. Waszczak, *Inorg. Chem.*, **15**, 17 (1976).

(6) M. S. Whittingham and F. R. Gamble, *Mater. Res. Bull.*, **10**, 363 (1975).

(7) G. A. Wiegers and C. F. van Bruggen, *Physica*, **86–88B**, 1009 (1977).

(8) B. van Laar and D. J. W. Ijdo, *J. Solid State Chem.*, **3**, 590 (1971).

(9) J. Rouxel, *J. Solid State Chem.*, **17**, 223 (1976).

(10) S. Brunie and M. Chevreton, *C. R. Hebd. Seances Acad. Sci.*, **258**, 5847 (1964).

(11) M. Danot, J. Bichon and J. Rouxel, *Bull. Soc. Chim. Fr.*, 3063 (1972).

(12) J. A. Wilson, F. J. Di Salvo, and S. Mahajan, *Adv. Phys.*, **24**, 117 (1975).

(13) J. P. Pouget, P. Lederer, D. S. Schreiber, H. Launois, D. Wohlleben, A. Casalot, and G. Villeneuve, *J. Phys. Chem. Solids*, **33**, 1961 (1972).

(14) A. C. Gossard, F. J. Di Salvo, L. R. Erick, J. P. Remeika, H. Yasuoha, K. Kosuge, and S. Kachi, *Phys. Rev. B.*, **10**, 4178 (1974).

(15) A. C. Gossard, J. P. Remeika, T. M. Rice, H. Yasuoha, K. Kosuge, and S. Kachi, *Phys. Rev. B.*, **9**, 1230 (1974).

(16) A. C. Gossard, A. Menth, W. W. Warren, and J. P. Remeika, *Phys. Rev. B*, **12**, 1187 (1975).

(17) F. J. Di Salvo and J. V. Waszczak, *J. Phys. (Paris), Colloq.*, **C4**, 157 (1976).

(18) P. M. Williams in "Crystallography and Crystal Chemistry of Materials with Layered Structures", Vol. 2, F. Levy, Ed., Reidel, Holland, 1976.

(19) C. F. van Bruggen and C. Haas, *Solid State Commun.*, **20**, 251 (1976).

(20) A. H. Thompson, *Phys. Rev. Lett.*, **34**, 520 (1975).

(21) J. R. Bloembergen, R. Haange, G. A. Wiegers, and C. F. van Bruggen, Extended Abstracts, Vth International Conference on Solid Compounds of Transition Elements, Uppsala, 1976, p 60.

(22) D. W. Murphy, J. N. Carides, F. J. Di Salvo, C. Cros, and J. V. Waszczak, *Mater. Res. Bull.*, **12**, 825 (1977).

Contribution No. 5609 from the Arthur Amos Noyes Laboratory of Chemical Physics,
California Institute of Technology, Pasadena, California 91125

Emission Spectra and Lifetimes of $Re_2Cl_8^{2-}$, $Re_2Br_8^{2-}$, and $Mo_2Cl_8^{4-}$ at 1.3 K upon Excitation of the $\delta \rightarrow \delta^*$ Transition

WILLIAM C. TROGLER, EDWARD I. SOLOMON, and HARRY B. GRAY*

Received May 10, 1977 AIC70341A

Excitation (650 nm) of $(n\text{-}Bu_4N)_2[Re_2Cl_8]$ and $(n\text{-}Bu_4N)_2[Re_2Br_8]$ in KBr disks at 1.3 K gives broad emission centered at 13 020 and 12 530 cm^{-1}, respectively. Emission lifetimes are as follows: $Re_2Cl_8^{2-}$, 150 ns; $Re_2Br_8^{2-}$, 110 ns. Luminescence was also recorded for the $Mo_2Cl_8^{4-}$ ion doped into a crystal of $(enH_2)Cl_2$. Again a broad, structureless emission band was observed (14 950 cm^{-1}, τ = 75 ns, 1.3 K). Owing to the lack of overlap of the emission with the 0–0 transition in absorption, it is proposed that the luminescent state is one of the spin–orbit components of $^3A_{2u}$. This places the $\delta \rightarrow \delta^*$ singlet–triplet splitting in the range 1000–3000 cm^{-1}.

Absorption spectroscopy has been employed to characterize the lowest spin-allowed transitions in compounds that contain a quadruple metal–metal bond.[1] With the exception of dimolybdenum(II) carboxylates,[2] the lowest singlet excited state in binuclear complexes of Mo(II) and Re(III) is $^1A_{2u}$ (in D_{4h} microsymmetry) derived from the one-electron excitation $\delta \rightarrow \delta^*$. The location of $^3A_{2u}(\delta \rightarrow \delta^*)$ (or, more properly, its A_{1u} and E_u spin–orbit components) in these complexes, however, has been the subject of some speculation. And, although scattered-wave Xα calculations have been performed for $Re_2Cl_8^{2-}$,[3] $Mo_2Cl_8^{4-}$,[4] and $Mo_2(O_2CH)_4$,[5] it is now recognized[5] that singlet–triplet splittings cannot be predicted reliably from this type of theory.

Clark and Franks[6] noticed a weak, structured absorption at 6250 cm^{-1} in the diffuse-reflectance spectra of some but not all of the $Mo_2Cl_8^{4-}$ salts they examined, and the suggestion was made that this near-IR band might be attributable to the $^1A_{1g} \rightarrow {}^3A_{2u}(\delta \rightarrow \delta^*)$ transition. However, it has been pointed out[7] that the 12 000-cm^{-1} singlet–triplet splitting that follows from such an interpretation is unexpectedly large, and the possibility of near-IR impurity absorption has been raised.[7,8] An alternative placement of $^1A_{1g} \rightarrow {}^3A_{2u}$ in $Mo_2Cl_8^{4-}$ could be 17 500 cm^{-1}, where Fanwick et al.[7] found a weak shoulder in one polarized absorption spectrum of a single crystal of $K_4Mo_2Cl_8 \cdot 2H_2O$ at 4 K.

In an attempt to gather more evidence concerning the position of the $^3A_{2u}$ state in quadruply bonded binuclear complexes, we have measured the emission spectra and lifetimes at 1.3 K of $(n\text{-}Bu_4N)_2[Re_2Cl_8]$, $(n\text{-}Bu_4N)_2[Re_2Br_8]$, and 0.2% $Mo_2Cl_8^{4-}$ in a single crystal of $(enH_2)Cl_2$. The results reported herein support a relatively small singlet–triplet splitting of the $\delta \rightarrow \delta^*$ excited states.

Experimental Section

The compounds $(n\text{-}Bu_4N)_2[Re_2Cl_8]$ and $(n\text{-}Bu_4N)_2[Re_2Br_8]$ were prepared by the literature method.[9] Crystals of $(enH_2)Cl_2$ doped with $Mo_2Cl_8^{4-}$ were prepared by the following modification of the literature synthesis[10] of $(enH_2)_2[Mo_2Cl_8]$. $Mo_2(O_2CCH_3)_4$[11] was added to a 6 N HCl solution saturated with $(enH_2)Cl_2$. The solution was filtered before slowly cooling to 5 °C, yielding a crop of translucent purple crystals. Anal. Calcd for $C_2H_{10}N_2Cl_2$: C, 17.9; H, 8.22; N, 20.9; Cl, 52.9. Found: C, 17.8; H, 7.48; N, 20.5; Cl, 54.1; Mo, 0.35. The Mo analysis corresponds to a mole fraction of $Mo_2Cl_8^{4-}$ of ca. 0.2% (assuming $Mo_2Cl_8^{4-}$ is the only Mo species present). The C, H, N, and Cl analyses were obtained from Chemalytics, Inc., Tempe, Ariz., and the Mo analysis was performed by Schwarzkopf Microanalytical Laboratory, Woodside, N.Y.

Emission spectra were obtained at the λ point of liquid He in an optical Dewar. A pulsed nitrogen laser was used to pump a dye laser (output pulse width of 32 ns) and excitation wavelengths of 650 and 540 nm were used for the Re(III) and Mo(II) compounds, respectively. Emission lifetimes were recorded at the wavelength of maximum